The Journal of Chemical Physics

Reactions of translationally cold trapped CCl^+ with acetylene (C_2H_2)

Cite as: J. Chem. Phys. **152**, 234310 (2020); https://doi.org/10.1063/5.0008656
Submitted: 23 March 2020 • Accepted: 31 May 2020 • Published Online: 19 June 2020

K. J. Catani, J. Greenberg, B. V. Saarel, et al.

View Online Export Citation CrossMark

ARTICLES YOU MAY BE INTERESTED IN

Isotope-specific reactions of acetonitrile (CH_3CN) with trapped, translationally cold CCl^+
The Journal of Chemical Physics **154**, 074305 (2021); https://doi.org/10.1063/5.0038113

A study of the translational temperature dependence of the reaction rate constant between CH_3CN and Ne^+ at low temperatures
The Journal of Chemical Physics **153**, 124305 (2020); https://doi.org/10.1063/5.0013807

Using isotopologues to probe the potential energy surface of reactions of $C_2H_2^+ + C_3H_4$
The Journal of Chemical Physics **154**, 124310 (2021); https://doi.org/10.1063/5.0046438

© 2020 Author(s).

The Journal of Chemical Physics ARTICLE scitation.org/journal/jcp

Reactions of translationally cold trapped CCl^+ with acetylene (C_2H_2)

Cite as: J. Chem. Phys. 152, 234310 (2020); doi: 10.1063/5.0008656
Submitted: 23 March 2020 • Accepted: 31 May 2020 •
Published Online: 19 June 2020

View Online Export Citation CrossMark

K. J. Catani,[a] J. Greenberg, B. V. Saarel, and H. J. Lewandowski

AFFILIATIONS

JILA and the Department of Physics, University of Colorado, Boulder, Colorado 80309-0440, USA

[a]Author to whom correspondence should be addressed: katherine.catani@colorado.edu

ABSTRACT

Ion–neutral chemical reactions are important in several areas of chemistry, including in some regions of the interstellar medium, planetary atmospheres, and comets. Reactions of CCl^+ with C_2H_2 are measured, and the main products include $C_3H_2^+$ and C_3H^+, both relevant in extraterrestrial environments. Accurate branching ratios are obtained, which favor the formation of $C_3H_2^+$ over C_3H^+ by a factor of four. The measured rate constants are on the order of Langevin, and complementary electronic structure calculations are used to aid in the interpretation of experimental results.

Published under license by AIP Publishing. https://doi.org/10.1063/5.0008656

I. INTRODUCTION

Chlorine containing compounds have been found to exist in extraterrestrial environments including the dense and diffuse clouds of the interstellar medium (ISM).[1–7] Interest in chlorine chemistry in these environments was initially fueled by detection of HCl, HCl^+, and H_2Cl^+ in these areas.[1–6] However, these small molecules are acknowledged to account for only a minor fraction of the overall chlorine abundance.[8–11] More recently, CH_3Cl was detected toward the low mass protostar IRAS 16293-2422 and comet Churyumov–Gerasimento.[7] Organohalogens, including CF^+, have been detected in these remote environments, but their overall chemical roles are not completely understood. A possible reservoir containing both carbon and chlorine is the carbon monochloride cation (CCl^+ shown in Fig. 1). CCl^+ has been proposed as an intermediate in the overall chlorine cycle in diffuse clouds, although its overall abundance is not known. The major predicted pathways to CCl^+ formation are through reactions of C^+ with HCl and H_2Cl.[8,9,12–17] Previous kinetic measurements, mainly using ion cyclotron resonance (ICR) spectrometry and selected ion flow tube (SIFT) techniques, found CCl^+ to be stable and non-reactive.[8,9,18] Products were observed for reactions with NH_3, H_2CO, CH_3Cl, $CHCl_3$, CCl_4, $CHCl_2F$, and $CHClF_2$.[8,9,18] However, with NO, H_2, CH_4, N_2, O_2, CO, and CO_2, no reactions were observed.[8,9,18] Although only a few reactions with relevant interstellar species have been measured, it is conceivable that CCl^+ could undergo reactive collisions with varying neutrals, such as acetylene (C_2H_2 shown in Fig. 1; previously detected and thought to be abundant).[19–23] Reactions of CCl^+ with neutral carbonaceous species would likely produce larger carbocation species.

Simple carbonaceous species like C_2H_2, c-$C_3H_2^+$, and l-C_3H^+ (observed cationic reaction products) have long been speculated to be present in the ISM. Recently, l-C_3H^+ was detected toward dark nebula in Orion and confirmed with laboratory spectroscopic measurements.[24–29] The role of $C_3H_2^+$ in these environments is less certain. Both neutral l-C_3H_2 and c-C_3H_2 have been detected toward dark clouds in the interstellar medium by their radioemission lines.[30] c-C_3H_2, in particular, has been detected in diffuse clouds, where ionizing radiation is more prevalent, and the role of its cation has been speculated as its probable precursor. Insight into additional formation pathways of these fundamental carbocations could prove useful for refining chemical models that rely on energetic and electronic information.

Understanding the details of these and other ion–neutral chemical reactions benefits from studies at low temperatures and is beginning to be explored using new experimental techniques. In particular, trapped Coulomb crystals have become increasingly popular as a way of studying cold ion–neutral chemical reactions.[31–40] Here, the reactant ion is sympathetically cooled to low translational temperatures by elastic collisions with co-trapped laser-cooled calcium ions. This technique allows for controlled interrogation of cold ion–neutral reactions at low pressures and temperatures over long timescales.

Published under license by AIP Publishing

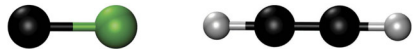

$CCl^+ X\,^1\Sigma^+$ $C_2H_2\ X\,^1\Sigma_g^+$

FIG. 1. Ground-state structures of CCl^+ and C_2H_2.

To characterize the CCl^+ cation and its reactivity in remote environments, we have measured the reactive pathways of gas-phase CCl^+ with C_2H_2 in a linear Paul ion trap coupled to a time-of-flight mass spectrometer (TOF-MS). The coupled ion trap enables co-trapping of sympathetically cooled CCl^+ with laser cooled Ca^+. This creates a controlled environment to study reactions with C_2H_2 that may be present in some areas of the ISM, planetary atmospheres, or comets. The reaction of $CCl^+ + C_2H_2$ leads to a possible pathway to the formation of c-$C_3H_2^+$ and l-C_3H^+ and to a measurement of the branching ratio of these two products. Complementary electronic structure calculations are used to aid in the discussion of the experimental results.

II. EXPERIMENTAL METHODS

Kinetic data for the reaction of $CCl^+ + C_2H_2$ were recorded at different interaction time steps by monitoring the masses of all ions present in a custom built linear Paul ion trap radially coupled to a TOF-MS. Details of the apparatus have been described previously,[33,39,41] and only a brief outline is presented here. CCl^+ was formed through non-resonant multiphoton ionization of tetrachloroethylene (TCE, C_2Cl_4). Vapor from TCE was seeded in a pulsed supersonic expansion of helium gas (3% TCE in ~1000 Torr He). The skimmed molecular beam was overlapped with 216 nm photons from a frequency-doubled, 10 Hz pulsed dye laser (LIOPTEC LiopStar; 10 ns pulse, 100 μJ/pulse) in the center of the ion trap forming $C^{35}Cl^+$, $C^{37}Cl^+$, C_2^+, C_2H^+, $^{35}Cl^+$, and $^{37}Cl^+$. Radio frequency (RF) secular excitation of contaminant ion masses was used to eject all cation species from the trap except $C^{35}Cl^+$ cations (subsequently denoted as CCl^+). Next, calcium was added to the chamber via effusive beam from a resistively heated oven and non-resonantly photoionized with 355 nm light from the third harmonic of a Nd:YAG laser (Minilite, 10 Hz, 7 mJ/pulse). Trapped calcium ions were Doppler laser cooled with two external cavity diode lasers (ECDLs) forming a Coulomb crystal composed of Ca^+ and a pure sample of CCl^+. Both ECDLs were fiber-coupled with one tuned to the $^2S_{1/2}$–$^2P_{1/2}$ transition of Ca^+ (397 nm; New Focus, 3.5 mW, 600 μm beam diameter) and the other to re-pump Ca^+ ions back into the cooling cycle on the $^2P_{1/2}$–$^2D_{3/2}$ transition (866 nm; New Focus, 9 mW, 600 μm beam diameter). Both laser frequencies were measured and locked using a wavemeter (HighFinesse/Ångstrom WSU-30).

Upon formation of a mixed-species Coulomb crystal, the RF trapping amplitude was dropped to allow any ions in metastable higher angular-momentum orbits to escape from the trap. This was repeated three times, leaving only cold Ca^+ and sympathetically cooled CCl^+. During the course of each experimental run, trapped Ca^+ ions were monitored continuously via their fluorescence using an intensified CCD camera. CCl^+ and other product ions do not fluoresce and were not directly seen in the images, but rather were inferred due to changes in the shape of the Coulomb crystal. Non-fluorescing ions were detected and quantified by ejecting the trapped species into a TOF-MS, which enabled unambiguous determination of the chemical formula based on the ion mass-to-charge ratio (m/z).

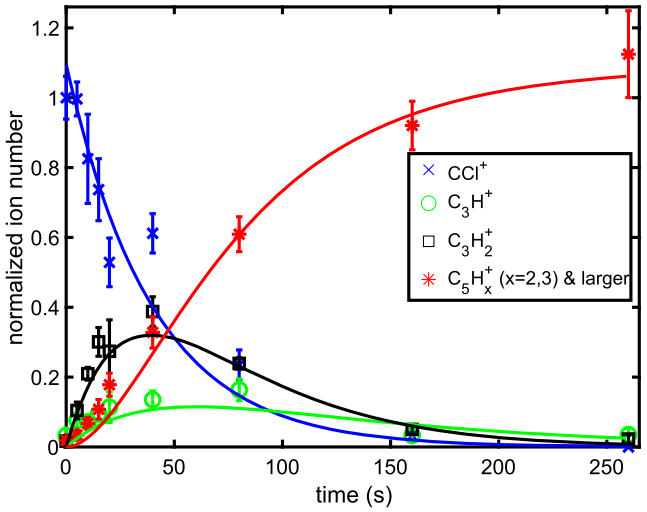

FIG. 2. Measured ion numbers of CCl^+ (blue crosses), C_3H^+ (green circles), $C_3H_2^+$ (black squares), and $C_5H_x^+$ (x = 2, 3, and higher; red asterisks) as a function of time. Data are normalized by the initial ion number of CCl^+ (~100). Each data point represents the mean and standard error from four experimental runs per time point. The averaged data are fit using a pseudo-first order reaction rate model (solid lines).

In a typical experimental run, ~100 CCl^+ ions (m/z 47) were loaded and sympathetically cooled by ~800 Ca^+ ions (m/z 40). Once the mixed Coulomb crystal was formed, neutral C_2H_2 (~4.7% in Ar at 298 K) was leaked into the vacuum system containing the trap at a constant pressure of ~$5(3) \times 10^{-9}$ Torr, measured using a Bayard–Alpert ion gauge, via a pulsed leak valve scheme.[42] The gas pulse duration was one of multiple neutral gas exposure time steps (0 s, 5 s, 10 s, 20 s, 40 s, 80 s, 160 s, and 260 s). At the end of each time step, a mass spectrum was measured, and ion numbers for each mass channel were recorded. An experimental run for every time step was repeated four times, and the number of ions from each mass channel of interest was averaged at each time step. Each mass channel of interest was normalized by the initial number of CCl^+ ions, and the average normalized ion numbers and standard error of the mean are plotted as a function of the different time steps as shown in Fig. 2.

III. COMPUTATIONAL METHODS

Structures, vibrational frequencies, and relaxed potential energy scans for $CCl^+ + C_2H_2$ were determined using the M06-2X/aug-cc-pVTZ level of theory. Potential energy surfaces were scanned along bond lengths, rotations, and angles to identify minima and saddle points. The M06-2X stationary points were used for coupled-cluster singles doubles (CCSD)/aug-cc-pVTZ calculations

Published under license by AIP Publishing

of structures and harmonic vibrational frequencies. The optimized structures were then used for single point energy calculations at the CCSD(T) level of theory with extrapolation to the complete basis set (CBS) limit using the aug-cc-pVXZ (X = T, Q) basis sets.[43–45] The energies were corrected for vibrational zero-point energy from the CCSD/aug-cc-pVTZ level of theory. Energies extrapolated to the CBS limit should account for possible basis set superposition errors. Structures for CCl^+ and C_2H_2 are shown in Fig. 1, with further geometric parameters and calculated harmonic vibrational frequencies (CCSD/aug-cc-pVTZ) provided in the supplementary material.

Other computational studies on CCl^+ itself recommend using multireference methods.[46–49] The computational cost of using multireference methods for the larger potential energy surface would be prohibitive, and therefore, we use the CCSD/aug-cc-pVTZ level of theory, which gives reasonable agreement with previously published computational and experimental data for CCl^+ and C_2H_2 separately.[46–50] Reported CCSD(T)/CBS//CCSD/aug-cc-pVTZ energies should be accurate to within 0.04 eV. Computations were compared to previous theoretical work and experimental data where available for the reactants and products in order to determine the best level of theory for accurate energetics. Density functional theory (DFT) and CCSD calculations were performed using both Gaussian 16 and Psi4 (version 1.3.2) computational packages.[51,52] Relaxed potential energy scans for the complexes at the M06-2X/aug-cc-pVTZ level of theory were undertaken using Gaussian 16.

IV. RESULTS AND DISCUSSION

A. $CCl^+ + C_2H_2$ reaction measurements

Using room temperature (298 K) C_2H_2, the average collision energy with translationally cold (~ 10 K) CCl^+ is 17 meV (~ 197 K). The excess collision energy should not be a significant source of energy to the reactions as the predicted products c-$C_3H_2^+ + Cl$ and l-$C_3H^+ + HCl$ are −0.15 eV and −0.07 eV exothermic, respectively [Eqs. (1) and (3)] based on CCSD(T)/CBS//CCSD/aug-cc-pVTZ level calculations,

$$CCl^+ + C_2H_2 \longrightarrow c\text{-}C_3H_2^+ + Cl \quad \Delta E = -0.15\,\text{eV}, \tag{1}$$

$$CCl^+ + C_2H_2 \longrightarrow l\text{-}C_3H_2^+ + Cl \quad \Delta E = 0.08\,\text{eV}, \tag{2}$$

$$CCl^+ + C_2H_2 \longrightarrow l\text{-}C_3H^+ + HCl \quad \Delta E = -0.07\,\text{eV}. \tag{3}$$

Several other product channels were explored theoretically, however, their endothermicities were significantly greater than the calculated average collision energy (greater than 1 eV above the reactant energies), and therefore, disqualified from the discussion of products. In addition, the l-$C_3H_2^+$ isomer could possibly contribute to the m/z 38 signal, however, the pathway is endothermic by about 0.08 eV, making it unlikely to be formed [see Eq. (2) discussed further in Sec. IV B 1].

As shown in Fig. 2, the initial ionic products that are formed as CCl^+ reacts away are indeed C_3H^+ and $C_3H_2^+$ (m/z 37 and 38, respectively). At about 40 s, the rates into the primary product C_3H^+ and $C_3H_2^+$ species are overtaken by the rates of these primary products reacting with the excess C_2H_2 present. This is illustrated by the turning over of the two corresponding curves (green and black traces) and growth of the secondary products of larger carbonaceous species (red trace), mainly comprising $C_5H_2^+$ and $C_5H_3^+$. The red trace plotted in Fig. 2 includes all mass channels above m/z 61, which should account for any secondary and tertiary (or larger) reaction products. Additions of C_2H_2 to $C_3H_x^+$ (x = 1, 2) have been characterized previously and are not modeled computationally.[53–57]

Experimental reaction rates are determined by fitting the reaction data, as shown in Fig. 2, to a pseudo-first-order reaction rate model; the fits are represented by solid lines. For the formation of primary and secondary products, the model is explicitly defined as

$$\frac{d[CCl^+]}{dt} = -(k_{37} + k_{38})[CCl^+], \tag{4}$$

$$\frac{d[C_3H^+]}{dt} = k_{37}[CCl^+] - k_{37\_63}[C_3H^+], \tag{5}$$

$$\frac{d[C_3H_2^+]}{dt} = k_{38}[CCl^+] - k_{38\_63}[C_3H_2^+], \tag{6}$$

$$\frac{d[C_5H_x^+]}{dt} = k_{37\_63}[C_3H^+] + k_{38\_63}[C_3H_2^+], \tag{7}$$

where the product ions of C_3H^+ (m/z 37), $C_3H_2^+$ (m/z 38), and $C_5H_x^+$ (x = 2, 3, and higher; $m/z \geq 62$) at time t are normalized with respect to the number of CCl^+ (~100) ions at $t = 0$. Rate constants are estimated using the measured concentration of neutral $C_2H_2 \approx 5(1) \times 10^6$ cm^3. It should be noted that the uncertainty quoted here is statistical. There is larger systematic uncertainty introduced by using an ion gauge in the 10^{-10} Torr regime. The resulting reaction rates and rate constants are given in Table I. These calculated rate constants are on the order of the rate calculated using Langevin collision theory, 1.1×10^{-9} cm^3 s^{-1}. The experimentally measured rate constant for CCl^+ reaction is still at least five times higher than that predicted by Langevin. It is possible that this reaction is not fully described using Langevin collision theory, but it is more likely that this discrepancy is due to the systematic inaccuracy of measuring neutral gas pressure using a hot cathode ion gauge around 10^{-10} Torr.[58] Even with this discrepancy, the measured relative rates for formation of $C_3H_2^+$ and C_3H^+ can still be used to determine an accurate branching ratio.

From the calculated rate constants, the branching ratio between the two primary products is determined to be about 4:1, with the Cl

TABLE I. Results from the fits to the pseudo-first order reaction rate models for the formation of primary and secondary products from the reaction of $CCl^+ + C_2H_2$. Included are the rate constants for the single pressure measurement of $C_2H_2 \approx 5(1) \times 10^6$ cm^3.

Species	m/z	k (s^{-1})	$k/(C_2H_2)$ (cm^3 s^{-1})
C_3H^+	37	$0.5(3) \times 10^{-2}$	$0.9(5) \times 10^{-9}$
$C_3H_2^+$	38	$2.0(3) \times 10^{-2}$	$4(1) \times 10^{-9}$
$C_5H_x^+$[a]	62 (and larger)	$4(1) \times 10^{-2}$	$6(2) \times 10^{-9}$

[a]Formation of $C_5H_x^+$ and higher order products from both $C_3H_2^+$ and C_3H^+.

Published under license by AIP Publishing

loss product channel (formation of $C_3H_2^+$) favored over the HCl loss product channel (formation of C_3H^+).

Further confirmation of the primary and secondary products was obtained by reaction of CCl^+ with deuterated acetylene (C_2D_2), where the product masses shifted to m/z 38 for C_3D^+ and m/z 40 for $C_3D_2^+$ as expected. Additionally, for both reactions with C_2H_2 and C_2D_2, the total ion numbers as a function of trap time were monitored to ensure conservation of trapped ions. These data are included in the supplementary material.

B. Modeling the $CCl^+ + C_2H_2$ reaction

In order to determine the relative energetics of the different pathways, an abridged potential energy surface of the $CCl^+ + C_2H_2$ reaction was explored; the key features of one possible reaction scheme that leads to the preferable primary products ($C_3H_2^+$ and C_3H^+) are shown in Fig. 3. Starting from the two reactants, at varying approaches, an intermediate complex can be exothermically formed, which should have excess internal energy [equilibrium structure is shown, 4.73 eV [CCSD(T)/CBS]]. Excess internal energy in the intermediate complex may be deposited into its vibrational modes, eventually leading to either Cl loss, through a barrierless dissociation, or HCl loss, which requires some rearrangement. Both channels are discussed in detail below. Geometric parameters (CCSD/aug-cc-pVTZ) and energies [CCSD(T)//CCSD/aug-cc-pVTZ] of each stationary point are given in the supplementary material.

1. Cl loss

One possible pathway, in which the reaction of $CCl^+ + C_2H_2$ proceeds, is through a low energy, though highly excited intermediate complex (equilibrium structure is shown as [2] in Fig. 3), which then leads to a barrierless dissociation into the favored products, c-$C_3H_2^+ + Cl$, residing ~0.15 eV below the reactants. The c-$C_3H_2^+$ isomer is favored over the l-$C_3H_2^+$ isomer by about 0.23 eV [22 kJ/mol; CCSD(T)/CBS//CCSD/aug-cc-pVTZ], and the barrier to rearrangement from linear to cyclic has been calculated in previous studies to be between 1.62 eV and 1.75 eV.[59] Indeed, it may be possible that both isomers are present, however, as noted above in Eq. (2), the l-$C_3H_2^+ + Cl$ products are slightly endothermic, by about 0.08 eV, making l-$C_3H_2^+$ unlikely to be formed. We assume the reactants have internal rotational energy corresponding to room temperature. A Boltzmann distribution at 300 K thus predicts ~11% of reactants have enough total energy to form l-$C_3H_2^+$. This pathway was not explicitly pursued in the current computational study. Future computational efforts could be invested in modeling this pathway, and possible future experimental work could focus on differentiating the potential isomers in each mass channel possibly using spectroscopic techniques. This would aid in further understanding the potential energy landscape of this reaction. Such investigations are beyond the scope of this work.

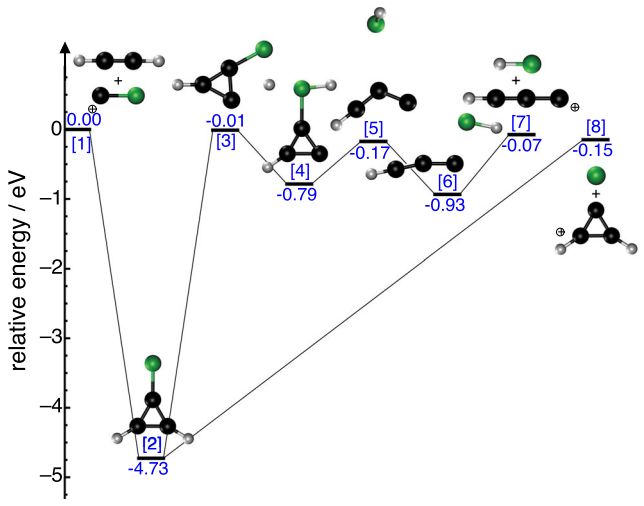

FIG. 3. The main features of the potential energy surface for one plausible reaction pathway of $CCl^+ + C_2H_2$ calculated at the CCSD(T)/CBS//CCSD/aug-cc-pVTZ level of theory. The favored Cl loss product, dissociates without a barrier, forming c-$C_3H_2^+ + Cl$ [8]. The HCl loss channel leading to l-$C_3H^+ + HCl$ [7] involves a few stationary points with lower energies than the dissociation limit of −0.1 eV. Here, the bare "+" indicates infinite separation.

2. HCl loss

The other primary product channel observed in the reaction of $CCl^+ + C_2H_2$ is the formation of C_3H^+ through HCl loss. Here, l-C_3H^+ is the only low energy isomer considered. This pathway goes through the same cyclic intermediate as the Cl loss channel ([2] in Fig. 3). From the cyclic structure, several rearrangements are required before eventually losing neutral HCl from l-C_3H^+. A few shallow minima were found where the HCl moiety rearranges along the conjugated pi-system of l-C_3H^+; the lowest energy isomer is shown ([6] in Fig. 3). The structures and energies of these different isomers are given in the supplementary material.

The experimentally observed branching ratio favors c-$C_3H_2^+$ over l-C_3H^+ by about a factor of four. In the absence of Rice–Ramsperger–Kassel–Marcus (RRKM) theory/master equation simulations, it is difficult to probe the potential energy surface barriers and their possible contribution to this observed branching ratio between the two primary product channels. The comparison is supported by the increased number of steps required for the HCl loss channel compared to the Cl loss channel. It should be noted that the barrier height of the H abstraction before HCl loss ([3] in Fig. 3) is variable based on the level of theory employed, with the CCSD(T)/CBS level giving the largest barrier. The uncertainty in the level of theory (0.04 eV) could push this barrier slightly endothermic, which would further kinetically favor the Cl loss channel.

V. CONCLUSIONS

The reaction of C_2H_2 with sympathetically cooled CCl^+ was examined using a linear Paul ion trap coupled to a TOF-MS. Although CCl^+ has been previously predicted to be non-reactive, it is clear that collisions with C_2H_2 result in either Cl or HCl loss. The primary products formed from these two loss channels are the astrochemically relevant c-$C_3H_2^+$ (with possibly some contribution of l-$C_3H_2^+$) and l-C_3H^+, respectively. The rate constants measured for the formation of the two primary products are on the order of those predicted through Langevin modeling. Furthermore, the Cl loss channel, occurring through a barrierless dissociation pathway, is

Published under license by AIP Publishing

favored by a factor of four compared to the HCl loss channel, which requires several rearrangements before losing HCl.

The theoretical work presented in this study would benefit from further exploration at a higher level of theory, possibly with multireference methods to characterize CCl^+ and its initial complexation with C_2H_2. In addition, kinetic modeling, possibly using RRKM theory, would be beneficial for a comprehensive comparison to experimentally measured branching ratios.

In the future work, we plan to explore further the reactivity of CCl^+ with other astrochemically relevant neutrals. In addition, a natural extension to this work would be to study similar reactions of CCl^+ with more control over the neutral reactant, using state-selected neutral molecules from a traveling wave Stark decelerator.[60,61] This will allow further study of ion–neutral reactions in low temperature regimes, where the internal quantum states and external motion can be controlled with high precision.

SUPPLEMENTARY MATERIAL

See the supplementary material for the following: (i) reaction curves from reactions of CCl^+ + acetylene (C_2H_2) and CCl^+ + deuterated acetylene (C_2D_2); (ii) measured total ion numbers (a sum of all detected ion channels in a given TOF-MS trace) for each reaction; (iii) full calculated potential energy surface at the CCSD/aug-cc-pVTZ level of theory with additional structural and energetic information provided for each stationary point.

ACKNOWLEDGMENTS

This work was supported by the National Science Foundation (Grant Nos. PHY-1734006 and CHE-1900294) and the Air Force Office of Scientific Research (Grant No. FA9550-16-1-0117).

DATA AVAILABILITY

The data that support the findings of this study are available within the article (and its supplementary material) and from the corresponding author upon reasonable request.

REFERENCES

[1]J. Zmuidzinas, G. A. Blake, J. Carlstrom, J. Keene, and D. Miller, Astrophys. J. **447**, L125 (1995).
[2]D. C. Lis, J. C. Pearson, D. A. Neufeld, P. Schilke, H. S. P. Müller, H. Gupta, T. A. Bell, C. Comito, T. G. Phillips, E. A. Bergin, C. Ceccarelli, P. F. Goldsmith, G. A. Blake, A. Bacmann, A. Baudry, M. Benedettini, A. Benz, J. Black, A. Boogert, S. Bottinelli, S. Cabrit, P. Caselli, A. Castets, E. Caux, J. Cernicharo, C. Codella, A. Coutens, N. Crimier, N. R. Crockett, F. Daniel, K. Demyk, C. Dominic, M.-L. Dubernet, M. Emprechtinger, P. Encrenaz, E. Falgarone, A. Fuente, M. Gerin, T. F. Giesen, J. R. Goicoechea, F. Helmich, P. Hennebelle, T. Henning, E. Herbst, P. Hily-Blant, Å. Hjalmarson, D. Hollenbach, T. Jack, C. Joblin, D. Johnstone, C. Kahane, M. Kama, M. Kaufman, A. Klotz, W. D. Langer, B. Larsson, J. Le Bourlot, B. Lefloch, F. Le Petit, D. Li, R. Liseau, S. D. Lord, A. Lorenzani, S. Maret, P. G. Martin, G. J. Melnick, K. M. Menten, P. Morris, J. A. Murphy, Z. Nagy, B. Nisini, V. Ossenkopf, S. Pacheco, L. Pagani, B. Parise, M. Pérault, R. Plume, S.-L. Qin, E. Roueff, M. Salez, A. Sandqvist, P. Saraceno, S. Schlemmer, K. Schuster, R. Snell, J. Stutzki, A. Tielens, N. Trappe, F. F. S. van der Tak, M. H. D. van der Wiel, E. van Dishoeck, C. Vastel, S. Viti, V. Wakelam, A. Walters, S. Wang, F. Wyrowski, H. W. Yorke, S. Yu, J. Zmuidzinas, Y. Delorme, J.-P. Desbat, R. Güsten, J.-M. Krieg, and B. Delforge, Astron. Astrophys. **521**, L9 (2010).
[3]D. A. Neufeld, E. Roueff, R. L. Snell, D. Lis, A. O. Benz, S. Bruderer, J. H. Black, M. De Luca, M. Gerin, P. F. Goldsmith, H. Gupta, N. Indriolo, J. Le Bourlot, F. Le Petit, B. Larsson, G. J. Melnick, K. M. Menten, R. Monje, Z. Nagy, T. G. Phillips, A. Sandqvist, P. Sonnentrucker, F. van der Tak, and M. G. Wolfire, Astrophys. J. **748**, 37 (2012).
[4]M. Goto, T. Usuda, T. R. Geballe, K. M. Menten, N. Indriolo, and D. A. Neufeld, Astron. Astrophys. **558**, L5 (2013).
[5]S. Muller, J. H. Black, M. Guelin, C. Henkel, F. Combes, M. Gérin, S. Aalto, A. Beelen, J. Darling, C. Horellou, S. Martín, K. M. Menten, D. V-Trung, and M. A. Zwaan, Astron. Astrophys. **566**, L6 (2014).
[6]D. A. Neufeld, J. H. Black, M. Gerin, J. R. Goicoechea, P. F. Goldsmith, C. Gry, H. Gupta, E. Herbst, N. Indriolo, D. Lis, K. M. Menten, R. Monje, B. Mookerjea, C. Persson, P. Schilke, P. Sonnentrucker, and M. G. Wolfire, Astrophys. J. **807**, 54 (2015).
[7]E. C. Fayolle, K. I. Öberg, K. I. Öberg, J. K. Jørgensen, K. Altwegg, H. Calcutt, H. S. P. Müller, M. Rubin, M. H. D. van der Wiel, P. Bjerkeli, T. L. Bourke, A. Coutens, E. F. van Dishoeck, M. N. Drozdovskaya, R. T. Garrod, N. F. W. Ligterink, M. V. Persson, S. F. Wampfler, J. J. Berthelier, J. De Keyser, B. Fiethe, S. A. Fuselier, S. Gasc, T. I. Gombosi, T. Sémon, C. Y. Tzou, and ROSINA Team, Nat. Astron. **1**, 703 (2017).
[8]D. Smith and N. G. Adams, Astrophys. J. **298**, 827 (1985).
[9]G. A. Blake, V. G. Anicich, and W. T. Huntress, Astrophys. J. **300**, 415 (1986).
[10]D. A. Neufeld and M. G. Wolfire, Astrophys. J. **706**, 1594 (2009).
[11]M. Lanza, Y. Kalugina, L. Wiesenfeld, A. Faure, and F. Lique, Mon. Not. R. Astron. Soc. **443**, 3351 (2014).
[12]V. G. Anicich, W. T. Huntress, Jr., and J. H. Futrell, Chem. Phys. Lett. **40**, 233 (1976).
[13]D. M. Sonnenfroh and J. M. Farrar, Astrophys. J. **335**, 491 (1988).
[14]C. E. Dateo and D. C. Clary, J. Chem. Phys. **90**, 7216 (1989).
[15]D. C. Clary, C. E. Dateo, and D. Smith, Chem. Phys. Lett. **167**, 1 (1990).
[16]J. Glosik, W. Freysinger, A. Hansel, P. Spanel, and W. Lindinger, J. Chem. Phys. **98**, 6995 (1993).
[17]J. Glosik, D. Smith, P. Španěl, W. Freysinger, and W. Lindinger, Int. J. Mass Spectrom. Ion Processes **129**, 131 (1993).
[18]V. G. Anicich, J. Phys. Chem. Ref. Data **22**, 1469 (1993).
[19]J. H. Lacy, N. J. Evans II, J. M. Achtermann, D. E. Bruce, J. F. Arens, and J. S. Carr, Astrophys. J. **342**, L43 (1989).
[20]F. Lahuis and E. F. van Dishoeck, Astron. Astrophys. **355**, 699 (2000).
[21]M. J. Mumma, M. A. DiSanti, N. Dello Russo, K. Magee-Sauer, E. Gibb, and R. Novak, Adv. Space Res. **31**, 2563 (2003).
[22]J. H. Waite, Jr., D. T. Young, T. E. Cravens, A. J. Coates, F. J. Crary, B. Magee, and J. Westlake, Science **316**, 870 (2007).
[23]M. Agúndez, J. Cernicharo, and J. R. Goicoechea, Astron. Astrophys. **483**, 831 (2008).
[24]J. Pety, P. Gratier, V. Guzmán, E. Roueff, M. Gerin, J. R. Goicoechea, S. Bardeau, A. Sievers, F. Le Petit, J. Le Bourlot, A. Belloche, and D. Talbi, Astron. Astrophys. **548**, A68 (2012).
[25]S. Brünken, L. Kluge, A. Stoffels, O. Asvany, and S. Schlemmer, Astrophys. J. **783**, L4 (2014).
[26]P. Botschwina, C. Stein, P. Sebald, B. Schröder, and R. Oswald, Astrophys. J. **787**, 72 (2014).
[27]V. V. Guzmán, J. Pety, J. R. Goicoechea, M. Gérin, E. Roueff, P. Gratier, and K. I. Öberg, Astrophys. J. **800**, L33 (2015).
[28]B. A. McGuire, Astrophys. J. Suppl. Ser. **239**, 17 (2018).
[29]M. Gérin, H. Liszt, D. Neufeld, B. Godard, P. Sonnentrucker, J. Pety, and E. Roueff, Astron. Astrophys. **622**, A26 (2019).
[30]P. Thaddeus, J. M. Vrtilek, and C. A. Gottlieb, Astrophys. J. **299**, L63 (1985).
[31]Y.-P. Chang, K. Długołęcki, J. Küpper, D. Rösch, D. Wild, and S. Willitsch, Science **342**, 98 (2013).
[32]G. K. Chen, C. Xie, T. Yang, A. Li, A. G. Suits, E. R. Hudson, W. C. Campbell, and H. Guo, Phys. Chem. Chem. Phys. **21**, 14005 (2019).

Published under license by AIP Publishing

[33]J. Greenberg, P. C. Schmid, M. Miller, J. F. Stanton, and H. J. Lewandowski, Phys. Rev. A **98**, 032702 (2018).
[34]A. Kilaj, H. Gao, D. Rösch, U. Rivero, J. Küpper, and S. Willitsch, Nat. Commun. **9**, 2096 (2018).
[35]K. Okada, T. Suganuma, T. Furukawa, T. Takayanagi, M. Wada, and H. A. Schuessler, Phys. Rev. A **87**, 043427 (2013).
[36]L. S. Petralia, A. Tsikritea, J. Loreau, T. P. Softley, and B. R. Heazlewood, Nat. Commun. **11**, 173 (2020).
[37]P. Puri, M. Mills, C. Schneider, I. Simbotin, J. A. Montgomery, Jr., R. Côté, A. G. Suits, and E. R. Hudson, Science **357**, 1370 (2017).
[38]D. Rösch, S. Willitsch, Y.-P. Chang, and J. Küpper, J. Chem. Phys. **140**, 124202 (2014).
[39]P. C. Schmid, M. I. Miller, J. Greenberg, T. L. Nguyen, J. F. Stanton, and H. J. Lewandowski, Mol. Phys. **117**, 3036 (2019).
[40]T. Yang, A. Li, G. K. Chen, C. Xie, A. G. Suits, W. C. Campbell, H. Guo, and E. R. Hudson, Phys. Chem. Lett. **9**, 3555 (2018).
[41]P. C. Schmid, J. Greenberg, M. I. Miller, K. Loeffler, and H. J. Lewandowski, Rev. Sci. Instrum. **88**, 123107 (2017).
[42]C. Q. Jiao, D. R. A. Ranatunga, W. E. Vaughn, and B. S. Freiser, J. Am. Soc. Mass Spectrom. **7**, 118 (1996).
[43]D. E. Woon and T. H. Dunning, Jr., J. Chem. Phys. **98**, 1358 (1993).
[44]R. A. Kendall, T. H. Dunning, Jr., and R. J. Harrison, J. Chem. Phys. **96**, 6796 (1992).
[45]A. Halkier, T. Helgaker, P. Jørgensen, W. Klopper, and J. Olsen, Chem. Phys. Lett. **302**, 437 (1999).
[46]Y. Nishimura, T. Mizuguchi, M. Tsuji, S. Obara, and K. Morokuma, J. Chem. Phys. **78**, 7260 (1983).
[47]K. A. Peterson and R. C. Woods, J. Chem. Phys. **87**, 4409 (1987).
[48]K. A. Peterson, R. C. Woods, P. Rosmus, and H. Werner, J. Chem. Phys. **93**, 1889 (1990).
[49]X. Zhang, H. Zhai, Y. Liu, and J. Sun, J. Quant. Spectrosc. Radiat. Transfer **119**, 23 (2013).
[50]M. Gruebele, M. Polak, G. A. Blake, and R. J. Saykally, J. Chem. Phys. **85**, 6276 (1986).
[51]M. J. Frisch, G. W. Trucks, H. B. Schlegel, G. E. Scuseria, M. A. Robb, J. R. Cheeseman, G. Scalmani, V. Barone, G. A. Petersson, H. Nakatsuji, X. Li, M. Caricato, A. V. Marenich, J. Bloino, B. G. Janesko, R. Gomperts, B. Mennucci, H. P. Hratchian, J. V. Ortiz, A. F. Izmaylov, J. L. Sonnenberg, D. Williams-Young, F. Ding, F. Lipparini, F. Egidi, J. Goings, B. Peng, A. Petrone, T. Henderson, D. Ranasinghe, V. G. Zakrzewski, J. Gao, N. Rega, G. Zheng, W. Liang, M. Hada, M. Ehara, K. Toyota, R. Fukuda, J. Hasegawa, M. Ishida, T. Nakajima, Y. Honda, O. Kitao, H. Nakai, T. Vreven, K. Throssell, J. A. Montgomery, Jr., J. E. Peralta, F. Ogliaro, M. J. Bearpark, J. J. Heyd, E. N. Brothers, K. N. Kudin, V. N. Staroverov, T. A. Keith, R. Kobayashi, J. Normand, K. Raghavachari, A. P. Rendell, J. C. Burant, S. S. Iyengar, J. Tomasi, M. Cossi, J. M. Millam, M. Klene, C. Adamo, R. Cammi, J. W. Ochterski, R. L. Martin, K. Morokuma, O. Farkas, J. B. Foresman, and D. J. Fox, Gaussian 16 Revision A.03, Gaussian Inc., Wallingford, CT, 2016.
[52]R. M. Parrish, L. A. Burns, D. G. A. Smith, A. C. Simmonett, A. E. DePrince III, E. G. Hohenstein, U. Bozkaya, A. Y. Sokolov, R. Di Remigio, R. M. Richard, J. F. Gonthier, A. M. James, H. R. McAlexander, A. Kumar, M. Saitow, X. Wang, B. P. Pritchard, P. Verma, H. F. Schaefer III, K. Patkowski, R. A. King, E. F. Valeev, F. A. Evangelista, J. M. Turney, T. D. Crawford, and C. D. Sherrill, J. Chem. Theory Comput. **13**, 3185 (2017).
[53]I. Szabo and P. J. Derrick, Int. J. Mass. Spectrom. and Ion Phys. **7**, 55 (1971).
[54]H. I. Schiff and D. K. Bohme, Astrophys. J. **232**, 740 (1979).
[55]V. G. Anicich, W. T. Huntress, Jr., and M. J. McEwan, J. Phys. Chem. **90**, 2446 (1986).
[56]D. Smith and N. G. Adams, Int. J. Mass Spectrom. Ion Phys. **76**, 307 (1987).
[57]S. W. McElvany, J. Chem. Phys. **89**, 2063 (1988).
[58]K. Jousten, CAS Cern Accelerator School, 2007.
[59]M. W. Wong and L. Radom, J. Am. Chem. Soc. **115**, 1507 (1993).
[60]Y. Shyur, N. J. Fitch, J. A. Bossert, T. Brown, and H. J. Lewandowski, Rev. Sci. Instrum. **89**, 084705 (2018).
[61]Y. Shyur, J. A. Bossert, and H. J. Lewandowski, J. Phys. B: At., Mol. Opt. Phys. **51**, 165101 (2018).

Published under license by AIP Publishing